

AD_____

Award Number: DAMD17-03-1-0742

TITLE: Identification of the Molecular Determinants of Breast Epithelial Cell Polarity

PRINCIPAL INVESTIGATOR: Masahiko Itoh, Ph.D.

CONTRACTING ORGANIZATION: University of California
Berkeley CA 94720

REPORT DATE: October 2006

TYPE OF REPORT: Final

PREPARED FOR: U.S. Army Medical Research and Materiel Command
Fort Detrick, Maryland 21702-5012

DISTRIBUTION STATEMENT: Approved for Public Release;
Distribution Unlimited

The views, opinions and/or findings contained in this report are those of the author(s) and should not be construed as an official Department of the Army position, policy or decision unless so designated by other documentation.

REPORT DOCUMENTATION PAGE				<i>Form Approved</i> OMB No. 0704-0188	
Public reporting burden for this collection of information is estimated to average 1 hour per response, including the time for reviewing instructions, searching existing data sources, gathering and maintaining the data needed, and completing and reviewing this collection of information. Send comments regarding this burden estimate or any other aspect of this collection of information, including suggestions for reducing this burden to Department of Defense, Washington Headquarters Services, Directorate for Information Operations and Reports (0704-0188), 1215 Jefferson Davis Highway, Suite 1204, Arlington, VA 22202-4302. Respondents should be aware that notwithstanding any other provision of law, no person shall be subject to any penalty for failing to comply with a collection of information if it does not display a currently valid OMB control number. PLEASE DO NOT RETURN YOUR FORM TO THE ABOVE ADDRESS.					
1. REPORT DATE (DD-MM-YYYY) 01/10/06		2. REPORT TYPE Final		3. DATES COVERED (From - To) 8 Sep 03 – 7 Sep 06	
4. TITLE AND SUBTITLE Identification of the Molecular Determinants of Breast Epithelial Cell Polarity				5a. CONTRACT NUMBER	
				5b. GRANT NUMBER DAMD17-03-1-0742	
				5c. PROGRAM ELEMENT NUMBER	
6. AUTHOR(S) IMasahiko Itoh, Ph.D. E-Mail: mitoh@dokkyomed.ac.jp				5d. PROJECT NUMBER	
				5e. TASK NUMBER	
				5f. WORK UNIT NUMBER	
7. PERFORMING ORGANIZATION NAME(S) AND ADDRESS(ES) University of California Berkeley CA 94720				8. PERFORMING ORGANIZATION REPORT NUMBER	
9. SPONSORING / MONITORING AGENCY NAME(S) AND ADDRESS(ES) U.S. Army Medical Research and Materiel Command Fort Detrick, Maryland 21702-5012				10. SPONSOR/MONITOR'S ACRONYM(S)	
				11. SPONSOR/MONITOR'S REPORT NUMBER(S)	
12. DISTRIBUTION / AVAILABILITY STATEMENT Approved for Public Release; Distribution Unlimited					
13. SUPPLEMENTARY NOTES					
14. ABSTRACT Maintenance of apico-basal polarity in normal breast epithelial acini requires a balance between cell proliferation and cell death and proper cell-cell and cell-extracellular matrix signaling. Aberrant regulation of any of these processes can disrupt tissue architecture and initiate tumor formation. We found that the small GTPase Rap1 is a crucial effector in the organization of acinar structure and the induction of lumen formation. Rap1 activity in malignant HMT-3522 T4-2 cells is appreciably higher than in their non-malignant counterparts, S1. Expression of dominant-negative Rap1 in T4-2 cells resulted in phenotypic reversion, that is, formation of acinar structures with correct apico-basal polarity, and dramatically reduced tumor incidence despite the persistence of genomic abnormalities. The Rap 1 revertants also featured prominent central lumina not observed when other reverting agents are used. Conversely, expression of dominant-active Rap1 in T4-2 cells inhibited phenotypic reversion and led to increased invasiveness. Thus, Rap1 acts as a central regulator of breast architecture, and instructs polarity during acinar morphogenesis.					
15. SUBJECT TERMS Polarity , Tissue architecture, Lumen formation, Rap 1					
16. SECURITY CLASSIFICATION OF:			17. LIMITATION OF ABSTRACT UU	18. NUMBER OF PAGES 23	19a. NAME OF RESPONSIBLE PERSON USAMRMC
a. REPORT U	b. ABSTRACT U	c. THIS PAGE U			19b. TELEPHONE NUMBER (include area code)

Table of Contents

Cover	1
SF 298	2
Table of Contents	3
Abstract.....	4
Introduction	4
Body	5
Conclusion	9
Key Research Accomplishments	10
Reportable Outcomes	11
References	11
Appendices	15

Abstract

Maintenance of apico-basal polarity in normal breast epithelial acini requires a balance between cell proliferation and cell death and proper cell-cell and cell-extracellular matrix signaling. Aberrant regulation of any of these processes can disrupt tissue architecture and initiate tumor formation. We found that the small GTPase Rap1 is a crucial effector in the organization of acinar structure and the induction of lumen formation. Rap1 activity in malignant HMT-3522 T4-2 cells is appreciably higher than in their non-malignant counterparts, S1. Expression of dominant-negative Rap1 in T4-2 cells resulted in phenotypic reversion, that is, formation of acinar structures with correct apico-basal polarity, and dramatically reduced tumor incidence despite the persistence of genomic abnormalities. The Rap1 revertants also featured prominent central lumina not observed when other reverting agents are used. Conversely, expression of dominant-active Rap1 in T4-2 cells inhibited phenotypic reversion and led to increased invasiveness. Thus, Rap1 acts as a central regulator of breast architecture, and instructs polarity during acinar morphogenesis.

Introduction

During normal development, integration of signals from the microenvironment, including cell-cell and cell-ECM adhesion signals, leads to establishment of tissue structure and apico-basal polarity (Bissell et al., 2005). Loss of normal tissue structure and polarity are hallmarks of tumor progression (Muthuswamy et al., 2001). To delineate the mechanisms regulating tissue polarity and its loss in breast cancer, we utilized an assay in which normal and malignant human breast epithelial cells are cultured within a physiologically relevant three-dimensional (3D) laminin-rich extracellular matrix (lrECM). In this assay, the non-malignant cell line HMT-3522 S1 (S1) form polarized and growth-arrested acini when cultured in 3D lrECM, resembling the structures formed by primary breast epithelial cells taken from reduction mammoplasty (Petersen et al., 1992). In contrast, their malignant counterpart, the HMT-3522 T4-2 (T4-2) cell line, forms highly proliferative, disorganized and apolar structures reminiscent of tumors *in vivo*. This is a good model to address how normal organ structure and function are maintained and how the balance is lost in cancer at the molecular level. Previous work in this laboratory showed that expression levels of EGFR, β 1-integrin, and their downstream effectors, including MAPK and PI3K, are increased in T4-2 compared to S1 cells, and downregulation of any of these signaling pathways in T4-2 cells cultured in 3D lrECM leads to growth arrest and reversion to a phenotype resembling normal polarized acini *in vivo* (Weaver et al., 1997). This project has been pursued to further characterize molecules and pathways involved in breast architecture through the regulation of epithelial polarity using the HMT-3522 model system.

Body

In the initial phase of this project, we sought to investigate tight junctions (TJs), one mode of cell-cell adhesion, since TJs play a critical role in regulation of epithelial polarity (Tsukita et al., 2001; Itoh and Bissell, 2003). The data obtained from experiments pertaining to **Task 1 (*Determine which tight junctions components are down/up regulated as human mammary epithelial cells proceed to malignancy*)** unexpectedly revealed that expression of TJ components is not altered between non-malignant S1 and malignant T4-2 cells cultured in 3D lrECM (Figure S1). In addition, significant differences in the structure of TJs and localization of their components were not observed between S1 and T4-2 cells (Figure S2), as we found in when completing **Task 2 (*Determine morphological features and localization pattern of tight junction (TJ) components in HMT-3522 series grown in 3D laminin-rich basement membrane with confocal and electron microscopy*)**. Therefore, we shifted the focus slightly to identify other candidate molecular mechanisms or pathways that might regulate polarity in our model system, and perhaps TJ components themselves. We then interrogated Rap1, a Ras superfamily small-G protein, as a potential polarity regulator in **Task 3 (*Examine gain and loss of function analyses*)** and in **Task 4 (*Determine gene expression profile in S1, T4-2, and reverted T4-2 cells using DNA microarray*)**. We also undertook **Task 5 (*Functional screening using expression cDNA library*)**, and generated an expression library using cDNA purified from S1 and T4-2 cells. Although we have not succeeded in obtaining positive clones thus far, this effort will be continued in our laboratory.

Lumen formation and acinar polarity are disrupted by Rap1 activation.

Rap1 is activated in response to a number of extracellular stimuli, including growth factors, cytokines, and cell-cell and cell-extracellular matrix (ECM) adhesion (Bos, 2005) . Like all G proteins, activation of Rap1 is mediated by specific guanine nucleotide exchange factors (GEFs), and in turn disrupted by GTPase activating proteins (GAPs). Active GTP-bound Rap1 functions through its many effectors, including the Rho GTPase family member, Rac1, to regulate inside-out signaling to integrins and cadherins and to control cytoskeletal structure, endothelial cell polarity, and differentiation. Despite its original discovery as an inhibitor of Ras-mediated transformation, Rap1 and its GEFs and GAPs have been found to be dysregulated in a variety of mouse and human cancers (Gao et al., 2006). Deregulating Rap1 activity by knocking out its GAP, Spa1, in mice leads to the development of myeloproliferative disorders mimicking human chronic myeloid leukemia, and overexpression of Rap1 induces oncogenic transformation in cultured fibroblasts. Additionally, the E6 protein of oncogenic human papillomavirus transforms cells in part by degrading the Rap1-GAP E6TP1. Because it both responds to and regulates cell-cell and cell-ECM adhesions, Rap1 is emerging as a key regulator of morphogenesis (Hattori et al., 2003).

We had found previously that malignant T4-2 cells (which form disorganized and apolar colonies when grown in 3D lrECM; Fig. 1A) showed appreciably higher levels of Rac1 activity relative to their nonmalignant S1 counterparts, and that down-modulation of Rac1 caused T4-2 cells to form polarized acinar structures without lumina (Liu et al.,

2004). Since Rac1 functions downstream of Rap1, we examined Rap1 activity in S1 and T4-2 cells using pull-down assays. Whereas the total level of Rap1 was similar in these two cell lines, the level of active GTP-bound Rap1 was appreciably higher in T4-2 than in S1 cells when cultured in 3D lrECM (Fig. 1B). As shown previously for a number of other signaling molecules in our system, this difference was observed only in 3D cultures and not in cells grown on tissue culture plastic, underscoring the importance of tissue context in regulation of signaling pathways.

Blocking Rap1 activity restores tissue polarity and induces lumen formation.

We asked whether down-modulating Rap1 could restore normal tissue architecture in malignant T4-2 cells. We established stable T4-2 transfectants that exogenously expressed dominant-negative Rap1 (T4-DN-Rap1) or vector only (T4-vector) as a control. T4-vector cells cultured in 3D lrECM behaved in a manner similar to untransfected cells, forming large disorganized colonies that could be induced to undergo phenotypic reversion with the EGFR inhibitor AG1478 (Fig. 1C). In sharp contrast, T4-DN-Rap1 cells had markedly different morphology in 3D lrECM, forming organized acinar structures similar to nonmalignant S1 cells even in the absence of the reverting agents (Fig. 1C). Indirect immunofluorescence of T4-DN-Rap1 and AG1478-treated acini showed correct localization of the basal marker $\alpha 6$ -integrin, the basolateral marker β -catenin, and the apical marker GM130 (a Golgi component that distributes to the apical side of the nucleus in polarized cells). In contrast, in control T4-vector colonies, $\alpha 6$ -integrin and β -catenin were distributed around the entire membrane of all cells and GM130 was randomly distributed, confirming that polarity was impaired. Therefore, expression of DN-Rap1 was sufficient to induce polarized acinar architecture in T4-2 cells in 3D lrECM.

Despite the fact that $\alpha 6$ -integrin, β -catenin, and GM130 could be induced to correctly localize by down-modulating of either EGFR or Rap1, we observed distinct differences between the resulting revertant acini. Throughout culture, T4-DN-Rap1 acini were twice as large as AG1478-treated T4-vector acini (Fig. 1D). Whereas inhibition of EGFR led to growth arrest by day 5, T4-DN-Rap1 cells continued to proliferate as assessed by a high percentage (~45%) of Ki67-positive acini remaining at day 8 of culture (Fig. 1D). The architectural differences between AG1478-treated vector acini and T4-DN-Rap1 acini became more evident by day 15 in 3D lrECM, at which time there were prominent lumina in greater than 60% of T4-DN-Rap1 acini but in fewer than 2% of AG1478-treated vector acini (Fig. 2A). Establishment of apical polarity involves creation of apical membrane domains associated with the presence of filamentous actin. We detected apically localized actin in T4-DN-Rap1 acini but not in AG1478-treated T4-vector acini (Fig. 2A), confirming once again that DN-Rap1 leads to the development of both apical and basal polarity in 3D lrECM.

Lumen formation is accompanied by apoptotic cell death within acinar structures (Debnath et al., 2002). Bim, a pro-apoptotic BH3-only Bcl-2 family protein, was identified as having a role in this process (Reginato et al., 2005). We examined apoptotic cell death *in situ* by indirect immunofluorescence for activated caspase-3; as expected,

apoptosis was restricted to those cells not in contact with basement membrane within T4-DN-Rap1 acini (Fig. 2A). Furthermore, western blotting of protein lysates from T4-DN-Rap1 acini demonstrated that Bim was upregulated at day 10 of culture (Fig. 2B). In contrast, we detected neither activated caspase-3 nor upregulation of Bim in AG1478-treated T4-vector acini. Thus normalization of Rap1 activity caused reversion of T4-2 cells with a resulting architecture comparable to that of non-malignant mammary epithelial cells, such as MCF-10A, which form lumina in 3D lrECM. The resulting acini form prominent lumina despite persistent proliferation, extending our laboratory's previous observation that normal tissue polarity can be uncoupled from growth control (Liu et al., 2004). These results suggest that formation of organized acinar structure by expressing DN-Rap1 in malignant T4-2 cells is achieved by increased apoptotic signaling within the center of the colonies.

Dominant-active Rap1 desensitizes T4-2 cells to reversion by treatment with EGFR inhibitors.

Whereas expression of DN-Rap1 reverted cells to a normal tissue polarity when cultured in 3D lrECM, stable T4-2 transfectants that exogenously expressed dominant-active Rap1 (T4-DA-Rap1) formed disorganized clusters phenotypically indistinguishable from controls (compare Fig. 1A to Fig. 3A). However, in the presence of AG1478, T4-DA-Rap1 cells failed to revert, forming large colonies with improperly localized $\alpha 6$ -integrin (Fig. 3A). Reverting T4-vector cells by treatment with AG1478 resulted in down-regulation of both EGFR and $\beta 1$ -integrin, as reported previously for wild type T4-2 cells (Wang et al., 1998). However, expression of these molecules was unaffected in AG1478-treated T4-DA-Rap1 cells (Fig. 3B). Expression of DA-Rap1 likewise blocked restoration of tissue polarity by treatment with concentrations of the function-blocking EGFR antibody mAb225 (2 μ g/ml; Fig. 3C) or the MAPK pathway inhibitor PD98059 (10 μ M; Fig. 3C) previously shown to revert wild type T4-2 cells. To determine if the resistance to inhibitors of the EGFR pathway was dose-dependent or absolute, we applied higher doses of AG1478, mAb225, or PD98059 and found that a 3-4-fold higher concentration of each antagonist was required to revert T4-DA-Rap1 cells than to revert the controls (Fig. 3C). In contrast, T4-DA-Rap1 cells were reverted successfully by standard treatment with the PI3K inhibitor LY294002 (Fig. 3C). These data suggest that expression of DA-Rap1 prevents T4-2 cells from sensing the 3D lrECM microenvironment, and results in an uncoupling of EGFR and $\beta 1$ -integrin signaling pathways analogous to T4-2 cells on tissue culture plastic.

Rap1 activity affects invasive phenotype of malignant T4-2 cells.

To explore whether these findings had relevance to tumor progression, we investigated invasiveness of both Rap1 transfectants in Matrigel-coated transwell chambers. We found that invasiveness correlated with Rap1 activity: invasion of T4-DN-Rap1 and T4-DA-Rap1 cells were 50% and 400% that of controls, respectively (Fig. 4).

MAPK and PI3K signaling are modulated by Rap1.

To dissect the molecular mediators of Rap1 signaling in 3D IrECM, we examined the expression and phosphorylation levels of downstream signaling molecules. Although T4-DA-Rap1 cells were resistant to reversion by AG1478, and T4-DN-Rap1 cells adopted normal tissue structure and polarity in the absence of EGFR inhibitors, we could detect no differences in the levels of active or total EGFR between the two transfectants (Fig. 5A). This is in contrast to cells reverted by small molecule inhibitors of EGFR or PI3K as well as β 1-integrin or EGFR inhibitory antibodies (Weaver et al, 1997; Wang et al, 1999; Liu et al., 2004). However, Erk1/2 and its target molecule p90RSK were more highly phosphorylated in T4-DA-Rap1 than in T4-DN-Rap1 cells or in controls, consistent with studies reporting activation of Erk1/2 by Rap1 (Gao et al., 2006), and consistent with our inability to revert them using standard concentrations of MEK inhibitor (Fig. 4C). Another MAPK family protein, p38, which was shown to be activated by Rap1 in neuronal cells, was unaffected, suggesting that Rap1 acts downstream of EGFR and upstream of Erk1/2 specifically in T4-2 cells.

To clarify the roles Rap1 and apoptotic mechanisms were playing in formation of the lumen in T4-DN-Rap1 cells, we measured the level of phosphorylated active Akt, which plays a central role in activating survival signals and suppressing death signals. We found that its level was greatly decreased in T4-DN-Rap1 cells (Fig. 5B). Phosphorylation of GSK3 β , a target of Akt, was similarly downregulated, whereas the PI3K antagonist PTEN was upregulated in T4-DN-Rap1 cells, indicating that PI3K signaling through Akt was decreased by expression of DN-Rap1. Unsurprisingly, we did not detect significant differences in the expression of phospho-Akt, phospho-GSK3 β , or PTEN in T4-DA-Rap1 cells compared to controls, consistent with our ability to revert them with similar doses of the PI3K inhibitor LY294002. We found that expression of the pro-apoptotic factor FOXO1 was reduced in T4-DA-Rap1 and increased in T4-DN-Rap1 cells at both the mRNA and protein levels (Fig. 5C), providing further evidence that cell death pathways were affected by Rap1 activity, and implicating FOXO1 in lumen formation in mammary epithelial cells. Thus, upregulated activity of Rap1, as is found in tumorigenic T4-2 cells, uncouples normal microenvironmental cues from apoptotic signaling, thereby inhibiting establishment of tissue polarity, lumen formation, and acinar morphogenesis.

Expression of genes involved in G2/M transition is affected by Rap1.

Since the analyses of 3D IrECM cultured T4-2 cells transfected with DA-Rap1 and DN-Rap1 showed that Rap1 plays a role in organizing polarity and tissue architecture via coordination of several signaling pathways, we underwent Task 4 using T4-vector, T4-DA-Rap1, and T4-DN-Rap1. RNA was isolated from these cells after culturing in 3D IrECM for 10 days and hybridized with Affymetrix DNA chips spotted with 22,000 human oligos. Obtained data were processed and analyzed with GeneSpring software.

484 genes are up-regulated and 361 genes are down-regulated more than 2-fold in T4-DA-Rap1 cells compared to T4-vector cells. Among 484 up-regulated genes, 162 genes were down-regulated in T4-DN-Rap1 cells, making these genes candidates for being

correlated with Rap1 activity in 3D lrECM culture (Fig. 6A). Several cell cycle regulators such as CyclinA2, CyclinB1, and CyclinB2 were identified and we confirmed these results with RT-PCR (Fig. 6B). Interestingly, all cyclins identified by microarray analysis were G2/M cyclins; G1/S cyclins such as CyclinD were not affected. In addition to these G2/M cyclins, a couple of genes playing a role in the G2 to M phase transition were up-regulated in T4-DA-Rap1 cells and down-regulated in T4-DN-Rap1 cells. A serine/threonine kinase Polo-like kinase-1 (Plk1) is one of them (Eckerdt et al., 2005). Plk1 is expressed from G2 onwards and is degraded at the end of mitosis. Although Plk1 is already present in G2, its kinase activity is first seen at the G2/M transition and reaches peak levels during mitosis. It was suggested that CyclinB-Cdk1 functions upstream of Plk1 and activates it. Up-regulation of cell cycle regulators is connected to progression of malignancy. For example, Plk1 is overexpressed in a various types of tumors and it is shown that expression level of Plk1 coincides with poor prognosis.

At the same time, amongst 361 down-regulated genes in T4-DA-Rap1 cells, 55 of these genes were up-regulated in T4-DN-Rap1 cells (Fig. 7A). Several membrane proteins (FLTR3, CD164, EphA3) with functions related to cell adhesion were identified, although their functional roles in the regulation of the tissue architecture of 3D lrECM cultured T4-2 cells has not yet been elucidated. As mentioned above, proapoptotic factor FOXO1 is significantly increased in T4-DN-Rap1 cells as compared to T4-DA-Rap1 cells (Fig. 7B). The proapoptotic activity of FOXO1 is mediated through the transcriptional regulation of several genes such as TRAIL, FasL, and Bim, which is a critical factor for lumen formation (Reginato et al., 2005). FOXO1 induces cell cycle arrest by transcriptional repression of positive cell cycle regulators, as well as transcriptional induction of negative cell cycle regulators such as p27, and thus FOXO1 plays a tumor suppressor-like role. Thus, down-regulation and up-regulation of FOXO1 in T4-DA-Rap1 and T4-DN-Rap1 cells, respectively, well correlates with their phenotype in 3D lrECM.

Conclusion

The functional unit of the mammary gland is the acinus, the establishment and maintenance of which depend on integration of cues from the surrounding microenvironment. A defining feature of the acinus is that its constituent cells are polarized, with distinct basolateral and apical membrane domains, surrounding a central lumen, which is required for secretion and storage of milk during lactation. One of the early events in breast cancer progression is the loss of the cues that maintain the lumen, i.e., aberrations in both apoptosis and autophagy. In this study, we identify Rap1 as a central modulator of lumen formation in breast epithelial cells, functioning upstream of the previously identified regulator Bim as well as several other pro-apoptotic molecules, including PTEN and FOXO1. The level of Rap1 activity correlates with the architecture of the acinus: if the level is appropriate, acini are formed; if it is too high, apoptosis is impaired, cells lose polarity, become mobile, and acinar lumens are filled.

Whereas inhibiting Rap1 activity restored tissue polarity and reduced tumorigenicity of T4-2 cells, high levels of Rap1 activity rendered cells resistant to reverting agents. These data underscore the notion that tissue polarity and malignancy are inversely related, but that tissue polarity and growth suppression are regulated by distinct pathways: here, cells expressing DN-Rap1 formed correctly polarized acini yet continued to proliferate more than their vector-transfected AG1478-reverted counterparts. These data, and our previously published work delineating the roles of Akt and Rac1 in proliferation and polarity downstream of PI3K, suggest that reversion of the malignant phenotype need not necessarily target deregulated proliferation if the treatment restores tissue architecture. Moreover, a polarized epithelial architecture has a protective effect, preventing malignancy even in cells with underlying genomic abnormalities.

Intriguingly, down-modulating Rap1 activity also down-modulated Akt signaling – as evaluated by levels of phospho-Akt, phospho-GSK3 β , and PTEN (Fig. 5B) – but had no effect on cell proliferation. These data are in contrast to reversion by treatment with the PI3K inhibitor LY294002, which also down-modulates signaling through both Akt and Rac1, but which leads to restoration of tissue polarity accompanied by growth modulation. One obvious difference between these two treatments is that PI3K inhibition leads to feedback modulation of both EGFR and β 1-integrin levels, whereas DN-Rap1 does not, suggesting either that PI3K and Rap1 are parallel pathways downstream of EGFR, or that Rap1 is activated independently of EGFR in tumorigenic T4-2 cells. In fact, DN-Rap1 is thus far the only reverting agent found that fails to normalize the activities of the other untreated pathways.

In conclusion, this study suggests that Rap1 functions as an organizer of breast acinar apical polarity and demonstrate that its dysregulation causes destruction of tissue architecture and leads to tumor progression. These findings indicate that signaling pathways mediated by Rap1 are potential new targets for breast cancer treatment.

Key Research Accomplishments

- GTP-bound active Rap1 is up-regulated in malignant T4-2 cells compared to non-malignant counterpart S1 cells in 3D lrECM context.
- Inhibiting Rap1 in malignant T4-2 cells does not cause growth arrest, but yields polarized acini distinct from the reverted structures obtained by AG1478 treatment.
- Apoptosis-mediated lumen formation is promoted in 3D lrECM cultured T4-2 cells by inhibition of Rap1.
- Dominant-active Rap1-expressing malignant T4-2 cells escape from growth suppression and morphological reversion by EGFR inhibitors.
- Invasive properties of malignant T4-2 cells are affected by Rap1 activity.

- Phenotypic alteration by Rap1 activity occurs independently from modulation of EGFR or β 1-integrin themselves.

Reportable Outcomes

- A manuscript including results described above entitled “**Rap1 integrates tissue polarity, lumen formation, and tumorigenic potential in human breast epithelial cells**” has been submitted to Cancer Research.
- Studies described above were presented at a minisymposium in the 45th annual meeting of the American Society for Cell Biology, 2005.
- Dr. Masahiko Itoh applied for and obtained an associate professor position at Dokkyo Medical University, Japan.

References

Bissell, M. J., Kenny, P. A., and Radisky, D. C. Microenvironmental regulators of tissue structure and function also regulate tumor induction and progression: the role of extracellular matrix and its degrading enzymes. *Cold Spring Harb Symp Quant Biol*, 70: 343-356, 2005.

Bos, J. L. Linking Rap to cell adhesion. *Curr Opin Cell Biol*, 17: 123-128, 2005.

Debnath, J., Mills, K. R., Collins, N. L., Reginato, M. J., Muthuswamy, S. K., and Brugge, J. S. The role of apoptosis in creating and maintaining luminal space within normal and oncogene-expressing mammary acini. *Cell*, 111: 29-40, 2002.

Eckerdt F, Yuan J, and Strebhardt K. Polo-like kinases and oncogenesis. *Oncogene*. 24(2):267-76, 2005.

Gao, L., Feng, Y., Bowers, R., Becker-Hapak, M., Gardner, J., Council, L., Linette, G., Zhao, H., and Cornelius, L. A. Ras-associated protein-1 regulates extracellular signal-regulated kinase activation and migration in melanoma cells: two processes important to melanoma tumorigenesis and metastasis. *Cancer Res*, 66: 7880-7888, 2006.

Hattori, M. and Minato, N. Rap1 GTPase: functions, regulation, and malignancy. *J Biochem (Tokyo)*, 134: 479-484, 2003.

Itoh, M. and Bissell, M.J. The organization of tight junctions in epithelia: implications for mammary gland biology and breast tumorigenesis. *J Mammary Gland Biol Neoplasia*. 8(4):449-62, 2003.

Liu, H., Radisky, D. C., Wang, F., and Bissell, M. J. Polarity and proliferation are controlled by distinct signaling pathways downstream of PI3-kinase in breast epithelial tumor cells. *J Cell Biol*, 164: 603-612, 2004.

Muthuswamy, S. K., Li, D., Lelievre, S., Bissell, M. J., and Brugge, J. S. ErbB2, but not ErbB1, reinitiates proliferation and induces luminal repopulation in epithelial acini. *Nat Cell Biol*, 3: 785-792, 2001.

Petersen, O. W., Ronnov-Jessen, L., Howlett, A. R., and Bissell, M. J. Interaction with basement membrane serves to rapidly distinguish growth and differentiation pattern of normal and malignant human breast epithelial cells. *Proc Natl Acad Sci U S A*, 89: 9064-9068, 1992.

Reginato, M.J., Mills, K.R., Becker, E.B., Lynch, D.K., Bonni, A., Muthuswamy, S.K., and Brugge, J.S. Bim regulation of lumen formation in cultured mammary epithelial acini is targeted by oncogenes. *Mol Cell Biol*. 25(11):4591-601, 2005.

Tsukita, S., Furuse, M., and Itoh, M. Multifunctional strands in tight junctions. *Nat Rev Mol. Cell Biol*. 2(4): 285-293, 2001.

Weaver, V. M., Petersen, O. W., Wang, F., Larabell, C. A., Briand, P., Damsky, C., and Bissell, M. J. Reversion of the malignant phenotype of human breast cells in three-dimensional culture and in vivo by integrin blocking antibodies. *J Cell Biol*, 137: 231-245, 1997.

Wang, F., Weaver, V.M., Petersen, O.W., Larabell, C.A., Dedhar, S., Briand, P., Lupu, R., and Bissell, M.J. Reciprocal interactions between beta1-integrin and epidermal growth factor receptor in three-dimensional basement membrane breast cultures: a different perspective in epithelial biology. *Proc Natl Acad Sci U S A*. 95(25):14821-14826, 1998.

Supporting Data

Figure Legends

Figure 1. Downregulation of Rap1 activity in malignant T4-2 cells restores tissue polarity in 3D lrECM culture. (A) Phase-contrast images of S1 and T4-2 cells cultured in 3D lrECM. (B) Rap1 expression and activity levels in S1 and T4-2 cells. Bar, 10 μ m. (C) Morphology of T4-vector treated with and without AG1478 and T4-DN-Rap1 colonies in 3D lrECM. Cell polarity was examined by staining markers for basal (α 6-integrin), basolateral (β -catenin), and apical (GM130) membrane domains. Bar, 5 μ m. (D) Cell proliferation in 3D lrECM was determined by measuring colony size (left) and Ki-67 positive colonies (right). Shown are averages and standard deviation across three independent experiments. (*) $p < 0.05$.

Figure 2. Bim-mediated lumen formation is induced in T4-DN-Rap1 cells but not in AG1478-treated control cells. (A) Phase contrast images after 15 days of culture in 3D lrECM, showing prominent lumina in T4-DN-Rap1 acini but not in AG1478-treated T4-vector acini. The localization of actin filaments in apical membrane domains confirmed lumen formation and establishment of apical polarity in T4-DN-Rap1 acini. Apoptotic cell death was examined by staining for active-caspase3 at day 10 of culture. (B) Expression level of Bim in T4-vector, AG1478-treated T4-vector, and T4-DN-Rap1 cells at day 10 of culture in 3D lrECM. Bar, 5 μ m.

Figure 3. T4-DA-Rap1 cells show dose-dependent resistance to reversion by inhibitors of EGFR and MAPK. (A) Phase-contrast images and immunofluorescence localization of α 6-integrin in T4-DA-Rap1 cells with or without 70nM AG1478 in 3D lrECM. (B) Levels of β 1-integrin, EGFR, and phospho-EGFR in 3D lrECM cultured T4-vector cells, and T4-DA-Rap1 cells in the presence and absence of 70nM AG1478. (C) Dose-dependent effect of reverting agents on T4-DA-Rap1 cells in 3D lrECM. Cells were treated with different doses of inhibitors against EGFR (AG1478 and mAb225), MEK (PD98059) or PI3K (LY294002). Bar, 5 μ m.

Figure 4. Level of Rap1 activity affects invasiveness of T4-2 cells. Invasiveness of T4-vector, T4-DA-Rap1, and T4-DN-Rap1 cells was examined using Matrigel-coated transwell filters. Quantification at 48 hr after plating.

Figure 5. Phenotype modulation caused by Rap1 occurs through different signaling pathways from those targeted by EGFR or β 1-integrin modulation. Activity and expression of the components of EGFR-MAPK pathway (A) and PTEN/Akt pathway (B) were examined by western blotting. (C) The levels of FOXO1 protein and mRNA were determined by western and RT-PCR analysis, respectively.

Figure 6. Genes up-regulated by dominant-active Rap1 and down-regulated by dominant-negative Rap1 in 3D lrECM cultured T4-2 cells. (A) RNA was isolated from 3D lrECM cultured T4-vector (vector), T4-DA-Rap1 (DA), and T4-DN-Rap1 (DN) cells for 10days. Isolated RNA was labeled and hybridized with Affymetrix human DNA oligo chips. Genes up-regulated more than 2-fold in T4-DA-Rap1 and down-regulated more than 2-fold in T4-DN-Rap1 cells as compared to T4-vector cells were chosen. (B) Expression of cell cycle regulator genes in the list were analyzed by RT-PCR.

Figure 7. Genes down-regulated by dominant-active Rap1 and up-regulated by dominant-negative Rap1 in 3D lrECM cultured T4-2 cells. (A) From the same data set in Figure 6, genes down-regulated more than 2-fold in T4-DA-Rap1 and up-regulated more than 2-fold in T4-DN-Rap1 cells as compared to T4-vector cells were chosen. (B) The array data was validated by RT-PCR regarding adhesion related molecules (FLRT3, CD164, EphA3).

Supplemental Figure Legends

Figure S1. Expression of tight junction components is not altered between S1 and T4-2 cells. Protein lysates were extracted from non-malignant S1 and malignant T4-2 cells cultured in 2D and 3D lrECM. Western blotting was performed using specific antibodies against tight junction components (ZO-1, ZO-2, PAR-3, MUPP1, aPKC, $G_{\alpha 12/13}$).

Figure S2. Electron microscopic images of HMT-3522 human mammary epithelial cells. (A) Non-malignant S1 and malignant T4-2 cells cultured on tissue culture plastic were fixed with 4% paraformaldehyde, embedded in Epon812, and ultrathin-sectioned. (B) S1, T4-2, and AG1478-treated T4-2 cells were cultured inside of Matrigel for 10 days. Cells were processed according to the same methods as 2D samples.

Figure 1

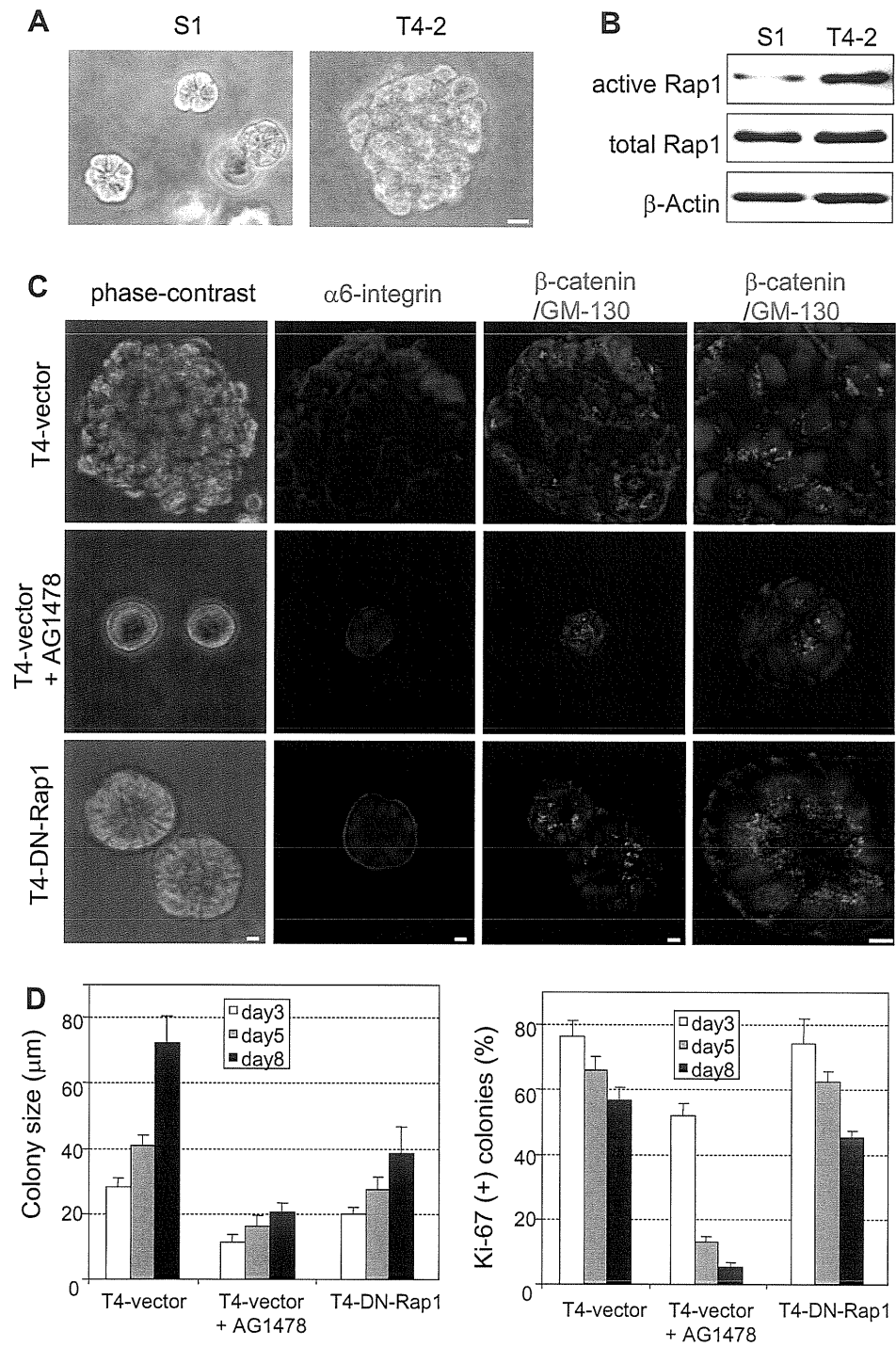


Figure 2

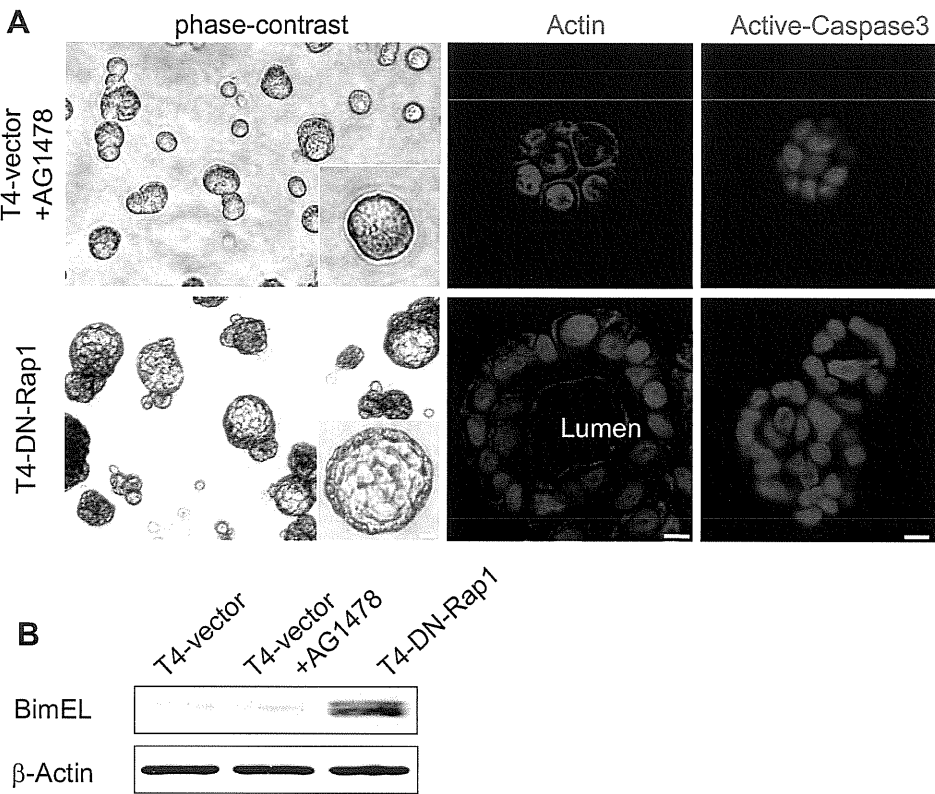


Figure 3

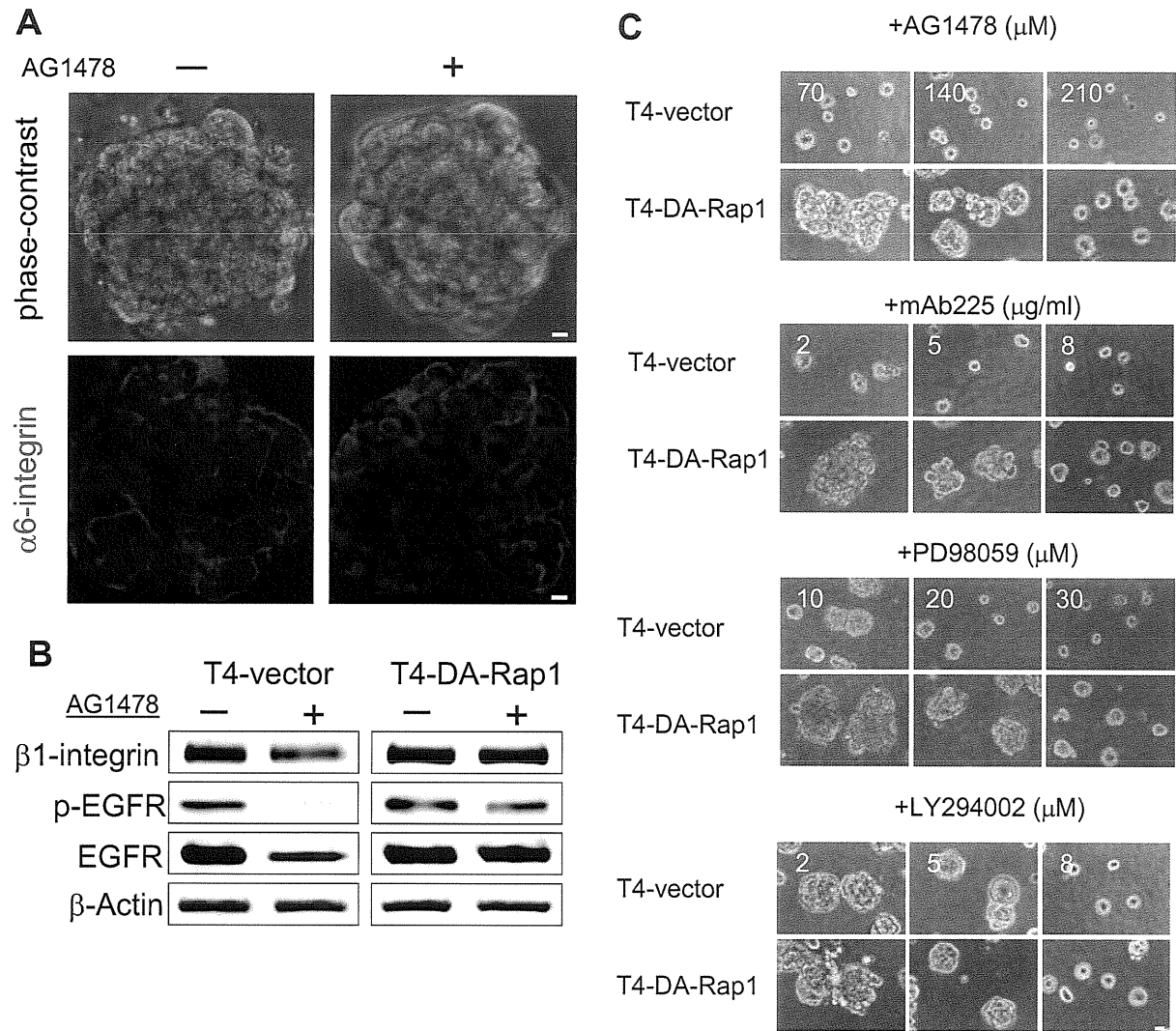


Figure 4

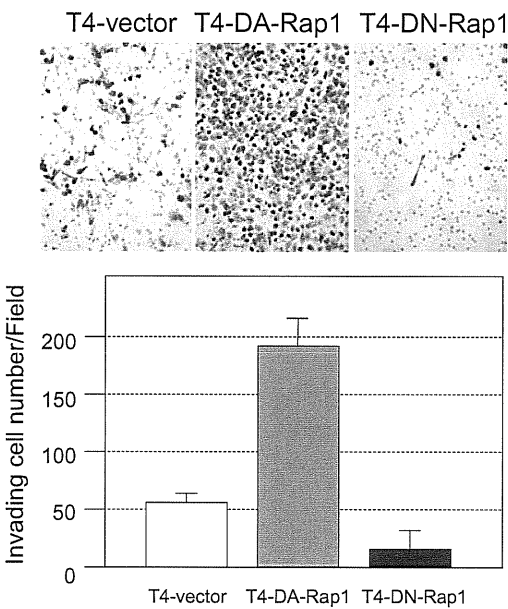


Figure 5

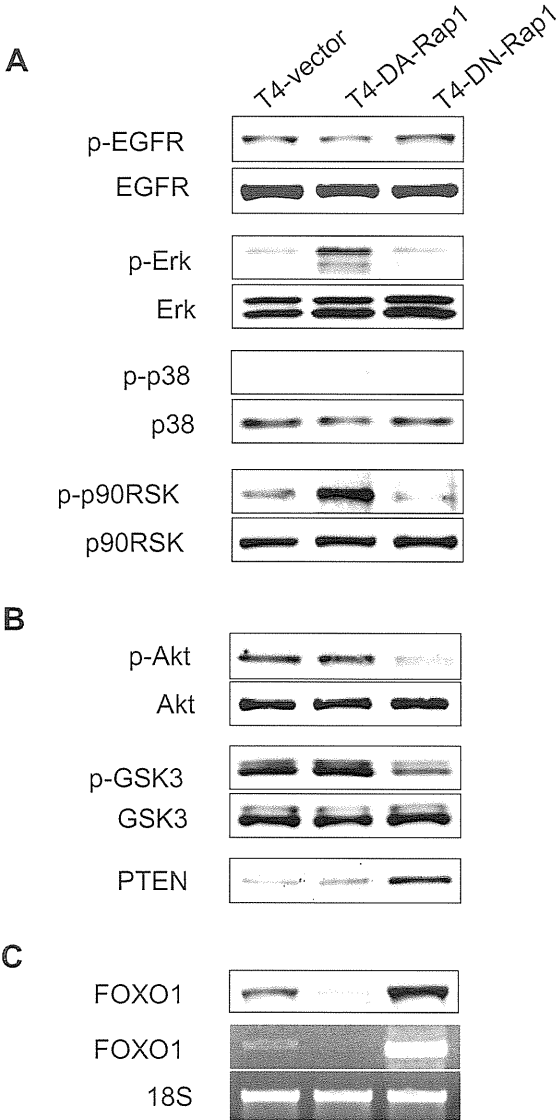


Figure 6

A	Relative Expression				
	Gene	vector	DA	DN	Tentative Functions
	CCNA2	1.0919973	2.6425416	0.053592324	cytokinesis; mitosis; mitotic G2 checkpoint
	TYMS	0.5480279	1.4277822	0.036987495	
	MKI67	0.8552262	2.5746226	0.06579376	
	HCAP-G	1.0215628	2.4948568	0.078790754	
	BUB1	0.9244152	2.0006654	0.07384517	cell cycle; mitosis; mitotic spindle checkpoint
	BIRC5	0.5966417	1.8545531	0.048084654	G2/M transition of mitotic cell cycle; anti-apoptosis
	DLG7	0.82783484	2.305587	0.070864715	cell-cell signaling
	CCNB2	0.87147295	2.120064	0.08310534	cytokinesis; mitosis; regulation of cell cycle
	ITGB6	1.5257393	3.8000565	0.15119849	cell-matrix adhesion; integrin-mediated signaling pathway
	KIF23	0.63200533	2.0384495	0.06445863	
	PRC1	0.85922474	1.858448	0.088264965	cell motility
	RAMP	0.4417453	1.1165247	0.0488256	
	HMMR	0.872858	2.1214485	0.10348793	
	KIF2C	1.1181177	2.410515	0.1351367	
	HCD	0.816046	2.2311494	0.09981128	cell proliferation; mitosis
	FOXMI	0.6544714	1.7568898	0.08130836	
	TOPK	0.5345668	1.2398124	0.06750798	regulation of transcription, DNA-dependent; protein amino acid phosphorylation
	SHCBP1	0.7688209	1.8113261	0.09726562	
	NEK2	0.9043545	1.8563162	0.115533575	
	CENPA	1.0519868	2.146762	0.13443993	
	BUB1B	0.748842	1.8407941	0.0959621	chromosome organization and biogenesis
	BM039	1.0119541	2.5257983	0.13072856	cell cycle; mitosis; mitotic checkpoint
	TTK	0.6439535	1.7277372	0.08524491	cell cycle; mitosis; mitotic checkpoint
	NUSAP1	0.63831764	1.4323531	0.08451068	
	ITGB6	1.2261727	2.9842029	0.16436659	
	TOP2A	0.6450744	1.5723388	0.08753789	
	CDC20	0.9665929	2.0321836	0.13187684	cell-matrix adhesion; integrin-mediated signaling pathway
	CCNB1	0.8328396	2.0190184	0.11442966	
	KIF2C	1.0239981	2.1265752	0.14333156	cytokinesis; mitosis; regulation of cell cycle;
	TOP2A	0.6239979	1.5876833	0.08759065	
	KIF14	0.83382434	2.1153696	0.11708649	
	MELK	0.9382825	2.3146737	0.13383737	
	PLK1	0.86326206	2.5722015	0.12395659	cell proliferation; mitosis
					protein amino acid phosphorylation
					mitosis; regulation of cell cycle

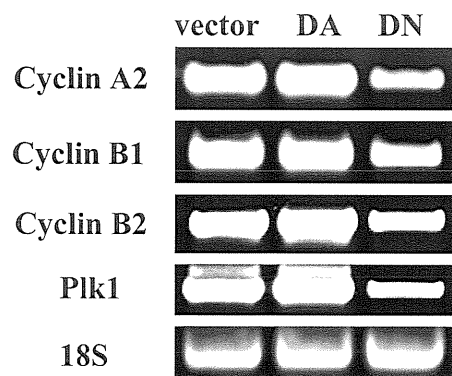
B

Figure 7

A

Gene	Relative Expression			Tentative Functions
	vector	DA	DN	
FLRT3	0.790824	0.103422	1.6006106	cell adhesion
FOXO1A	0.4757368	0.0796958	1.4303746	cell growth and/or maintenance
FOXO1A	0.4925211	0.0933921	1.3289582	
SSBP2	0.6277085	0.1281728	1.2609769	regulation of transcription
SFTPD	0.36057106	0.08233767	6.842762	alveolus development; antimicrobial humoral response
CHI3L1	0.71042913	0.16271149	12.270392	metabolism
GLUL	0.92143136	0.21382467	2.0767071	glutamine biosynthesis; regulation of neurotransmitter levels
PIK3R1	0.85376036	0.19904014	1.9414734	
EDN2	0.90809673	0.25050837	2.0687683	cell-cell signaling; pathogenesis; protein kinase C activation
ZNF117	1.385492	0.42278636	3.9010868	regulation of transcription, DNA-dependent
CHI3L1	0.7882396	0.24171974	13.36809	metabolism
PIK3R1	0.9270732	0.2915556	2.3769877	
BTN3A3	1.2455647	0.39832592	3.2908442	
DHRS3	1.1043123	0.35417378	2.4478369	fatty acid metabolism; visual perception
PIK3R1	0.8676907	0.28249344	2.1894214	
ZNF145	0.4386975	0.14296351	1.9047638	cell growth and/or maintenance; mesoderm development
SATB1	0.98099995	0.3377764	3.154174	establishment and/or maintenance of chromatin architecture
SAH	1.9256705	0.66484934	3.890238	
H15535	0.5413008	0.18692802	1.3262423	
LIMK2	0.91330034	0.317773	3.498192	
PLSCR4	0.7949644	0.28097877	2.6874092	blood coagulation; phospholipid scrambling
CYBRD1	0.9787124	0.35122323	3.3442028	electron transport
MGC5618	1.323369	0.4926617	3.7010477	
GBP2	0.527534	0.19711149	3.625249	immune response
CFLAR	1.4059851	0.52652043	2.9176702	induction of apoptosis by extracellular signals;
CFLAR	1.3396767	0.50927955	2.9352493	induction of apoptosis by extracellular signals
LIMK2	1.2721328	0.4895091	4.924092	
BTN3A3	1.1174442	0.43154046	3.293279	
CFLAR	1.2953199	0.50313205	3.1971414	induction of apoptosis by extracellular signals
SOD2	1.8470949	0.7515606	4.305439	response to oxidative stress; superoxide metabolism
IFIT1	0.7861041	0.32023448	3.48812	immune response
RNASE4	1.0720158	0.4436017	2.2065537	
EFEMP1	0.322507	0.13526835	2.5287693	visual perception

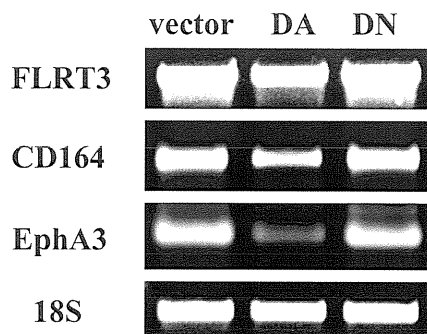
B

Figure S1

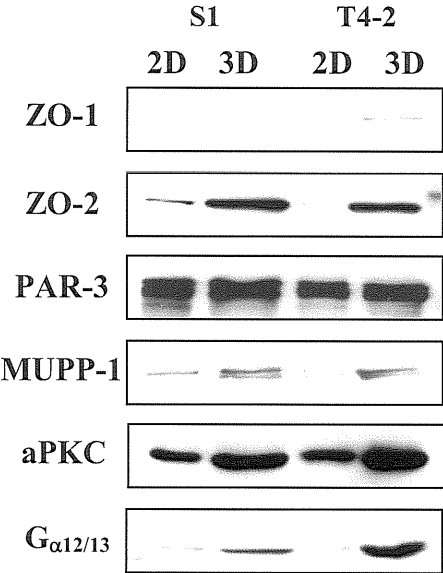
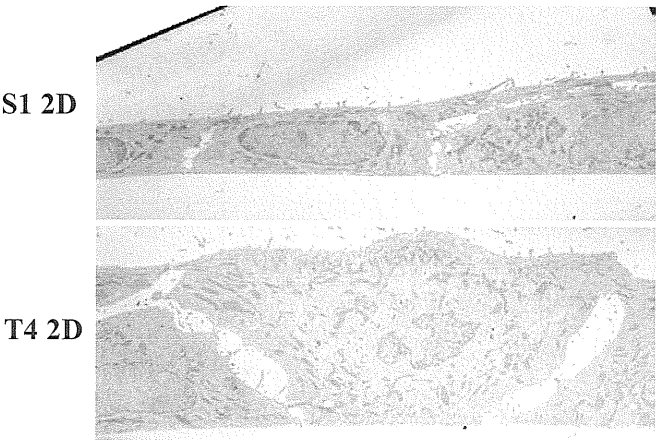


Figure S2

A



B

